RPE | Radiation Physics & Engineering
An International Peer-Reviewed Journal
Published by K.N. Toosi University of Technology
http://rpe.kntu.ac.ir
Research Article

Radiation Physics and Engineering 2021; 2(4):1–9
https://doi.org/10.22034/RPE.2021.303359.1039

The impact of neutronic safety parameters on SMART reactor dynamic response

Sarah Kamalpour[a], Hossein Khalafi[b,*]

[a] Department of Nuclear Engineering, Science and Research Branch, Islamic Azad University, Tehran, Iran
[b] Nuclear Science and Technology Research Institute (NSTRI), Tehran, Iran

HIGHLIGHTS

- Variation of neutronic safety parameters versus reactor cycle time is evaluated.
- Reactor behavior is analyzed under ramp reactivity insertion accident.
- Reactor dynamic response is predicted based on point kinetic equations and lumped temperature model.

ABSTRACT

The neutronic safety parameters determine reactor dynamic response. These parameters change as a function of core inventory during reactor cycle. Therefore, assessment of reactor behavior throughout operational cycle is an important issue in reactor safety analysis for transients. The purpose of the present study is to evaluate SMART reactor response to changes in neutronic safety parameters during reactor cycle in reactivity insertion accident condition. MCNPX2.6 nuclear code is utilized to calculate neutronic safety parameters throughout reactor cycle. The reactor dynamic model is simulated based on point kinetic equations and lumped temperatures to predict reactor response to ramp reactivity insertion. Based on this approach, the effect of neutronic parameters on reactor behavior are investigated in the beginning and end of cycle under reactivity transients. Hot full and zero power operational reactor states are considered in the analysis. Results illustrate that reactor at end of cycle has faster response with smaller transient power peak during reactivity insertion accident compared to beginning of cycle. The neutronic parameters, specifically negative feedbacks at both beginning and end of reactor cycle guarantee the safe performance of reactor at all examined conditions. The detailed comparative results are explained in the paper.

KEYWORDS

SMART
Dynamic Response
Reactivity Insertion Accident
Safety Parameters

HISTORY

Received: 07 September 2021
Revised: 31 October 2021
Accepted: 15 November 2021
Published: Autumn 2021

Nomenclature

β_{eff}	Effective delayed neutron fraction
k_{eff}	Effective multiplication factor
k_p	Prompt neutron effective multiplication factor
Λ	Neutron mean generation time
l_p	Prompt neutron lifetime
t	Time, the independent variable
$n_r(t)$	Time dependent relative neutron density
$C_i(t)$	i^{th} group of delayed neutron precursors
i	Delayed neutron group number ($i = 1, 2, \cdots, 6$)
$\beta_{\text{eff},i}$	i^{th} group of effective delayed neutron fractions
λ_i	i^{th} group delayed neutron decay constant
ρ	Reactivity
ρ_{inserted}	Inserted reactivity
$\rho_{\text{feedback}}(T_{\text{fave}}, T_{\text{Cool}})$	Total feedback reactivity which is a function of T_{fave} and T_{Cool}
P_0	Nominal reactor power
S_f	Deposition fraction of fission power in fuel
T_{fcenter}	Fuel center temperature
T_{fave0}	Average fuel temperature at normal operational condition
T_{fave}	Average fuel temperature
T_{Clad}	Average clad temperature
T_{Cool0}	Average coolant temperature at normal operational condition
T_{Cool}	Average coolant temperature
T_{in}	Core coolant inlet temperature
T_{out}	Core coolant outlet temperature
A_g	Heat transfer area of fuel gap
A_{Cool}	Heat transfer area of coolant
$\alpha_f T_{\text{fave}}$	Fuel temperature coefficient at T_{fave}

*Corresponding author: hkhalafi@aeoi.org.ir

$\alpha_{Cool}T_{Cool}$	Coolant temperature coefficient at T_{Cool}
h_{Cool}	Convection coefficient of the coolant
h_g	Heat conduction coefficient of the gap
C_f	Fuel material heat capacity
C_{Clad}	Clad material heat capacity
C_{Cool}	Coolant material heat capacity
M_f	Total fuel mass
M_{Clad}	Total mass of the clad
M_{Cool}	Total mass of the coolant
M^0_{Cool}	Coolant mass flow rate
BOC	Beginning of Cycle
EOC	End of Cycle
FTC	Fuel Temperature Coefficient
HFP	Hot Full Power
HZP	Hot Zero Power
MTC	Moderator Temperature Coefficient
RIA	Reactivity Insertion Accident
SMART	System-integrated Modular Advanced ReacTor

1 Introduction

Reactivity temperature coefficients and kinetic parameters are the main characteristics which determine the reactor state under transient conditions (Louis, 2021a). Upon reactor power change, the primary response is related to reactivity temperature coefficients. Negative fuel and moderator temperature coefficients stabilize the reactor power operation (CNSC, 2003). Kinetic parameters including effective delayed neutron fraction and neutron generation time are also key factors in safety analysis, since they have dominant influence on the reactor response time scale and also reactor power change rate (Louis, 2021b).

Several studies are performed for determining reactivity temperature coefficients and kinetic parameters as the main safety neutronic parameters. The effect of fuel material (Reda et al., 2021), temperature (Pinem et al., 2018), control rods (Torabi et al., 2018) and etc. on these parameters are also investigated.

Louis (Louis, 2021a) has studied the neutronic safety parameters of VVER-1000 core under various accident conditions. The author has concluded that reactor remains safe due to negative reactivity temperature coefficients and sufficient control rod worth under various accident conditions.

In another study (Louis, 2021b), sensitivity of kinetic parameters on variation of control rod movement, temperature changes, fuel consumption, fuel enrichment and burnable absorbers are investigated. The author reported that fuel burnup has the significant impact on effective delayed neutron fraction.

The main goal of the present study is to evaluate reactor response to changes in neutronic safety parameters during reactor cycle. For this purpose, several parameters including fuel composition, fuel and moderator temperature coefficients, effective delayed neutron fraction and neutron generation time are calculated during reactor cycle using MCNPX2.6 nuclear code (Pelowitz, 2008). An accurate prediction of these parameters is essential for reactor dynamics analysis.

Afterwards, the effect of neutronic safety parameters variation on reactor behavior is examined through dynamic model developed with MATLAB software (Hunt et al., 2014). A reactivity insertion accident is assessed in the beginning and end of cycle at both HFP and HZP reactor operational states.

2 SMART reactor core description

System-integrated Modular Advanced ReacTor (SMART) is selected as a case study. SMART is an advanced small modular reactor designed to produce 330 MW thermal power. The reactor core consists of 57 fuel assemblies with a standard 17×17 array. Each fuel assembly is loaded with 264 fuel rods, 24 control rod guide tubes and one instrumentation thimble (Ingersoll and Carelli, 2015). Figure 1 shows SMART reactor core configuration (Lee, 2010). The UO_2 pellets with enrichment lower than 5 w/o in Zircaloy cladding form the fuel rods. A sufficient amount of reactivity is provided in SMART for 36-month full power reactor operation. Excess reactivity is controlled by integral burnable absorbers, soluble boron and control rods. Reactor general specifications are given in Table 1.

3 Methods of calculation

The present study is performed in two steps. In the first step, neutronic safety parameters during reactor cycle are evaluated as follows:

- A detailed three-dimensional model of SMART reactor core is simulated by MCNPX2.6 nuclear code using ENDF-VI library. Criticality calculations are carried out by KCODE card. In this card, 104 neutron histories are traced in 9.9×10^3 active cycles. The first 10^2 cycles are skipped before history accumulation. Validation of SMART reactor simulation is performed in (Kamalpour et al., 2019).

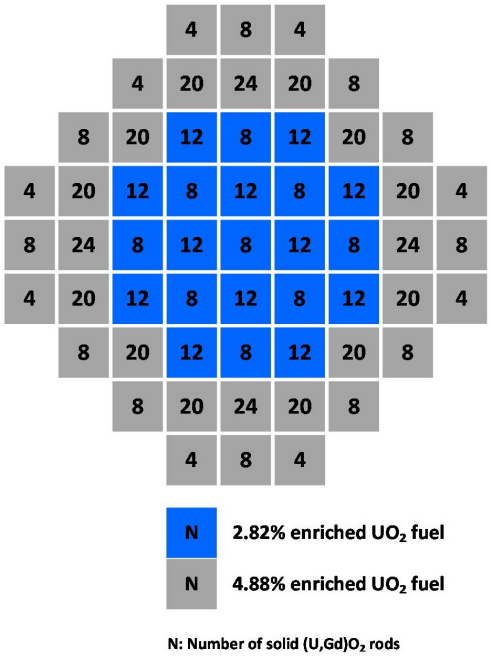

Figure 1: SMART reactor core design (Lee, 2010).

Table 1: SMART reactor specification (Ingersoll and Carelli, 2015).

Reactor Thermal Power	330 MW_{th}
Electrical Power	100 MW_e
Number of Fuel Assemblies	57
Lattice Geometry	Square
Active Core Height	2 m
Equivalent Core Diameter	1.382 m
Average Linear Heat Rate	10.97 $kW.m^{-1}$
Average Core Power Density	62.60 $MW.m^{-3}$
Fuel Cycle Length	3 years
Reactivity Control	Burnable Absorbers, Soluble Boron, Control Rods
Reactor Operating Pressure	15 MPa
Primary Coolant flow rate	2090 $kg.s^{-1}$
Core Coolant Inlet Temperature	568.8 K
Core Coolant Outlet Temperature	596.2 K

Table 2: FTC values in different temperature intervals.

Temperature intervals		FTC ($pcm.K^{-1}$)	
T1 (K)	T2 (K)	BOC	EOC
293	393	-5.71	-5.27
393	493	-2.47	-4.04
493	593	-2.27	-2.87
593	693	-2.02	-2.91
693	793	-1.95	-1.94
793	893	-1.79	-2.39
893	993	-1.85	-2.21
993	1093	-1.68	-2.01
1093	1193	-1.56	-1.74
1193	1293	-1.50	-2.57
1293	1393	-1.43	-1.75
11393	1593	-1.49	-1.54
1593	1793	-1.36	-1.85
Average (293 K-1793 K)		-1.94	-2.39

- The core inventory changes with reactor operation during cycle. In this regard, depletion calculations are implemented in assembly-wise approximation using BURN card. This card uses CINDER90 module to calculate burnable material densities and associated burnup at specified time steps (Stankovskiy and Van den Eynde, 2012). The SMART core inventory is calculated in 12 time steps for three years of reactor operation. In this assessment, the amount of fuel and integral burnable absorbers and consequently the core reactivity are obtained in each time step. The excess reactivity is essential to maintain criticality throughout reactor cycle. however, this excess reactivity should be suppressed for reactor safe operation. In this study, it is assumed that soluble boron keeps the reactor at critical state. The soluble boron concentration required for achieving criticality ($k_{\text{eff}} = 1$) in each step is calculated. Further parameters are calculated in the critical state with specified amount of soluble boron concentration.

- Temperature change in fuel or moderator causes reactivity change which is called feedback effect (CNSC, 2003). The fuel and moderator temperature coefficients (FTC & MTC) are calculated during reactor cycle. In order to calculate FTC, fuel temperature is changed from 293 K to 1773 K in 13 temperature intervals (refer to Table 2). MTC is also calculated by changing moderator temperature and subsequently moderator density within specified range of 293 K to 615 K in 7 temperature intervals (refer to Table 4). Constant temperature of 293 K is considered for other regions in the calculations. The temperature dependent cross sections for fuel and moderator are generated by NJOY nuclear cross section processing code (MacFarlane and Muir, 1994).

- The time scale of reactor response during transients depends on kinetic parameters. Kinetic parameters include effective delayed neutron fraction and neutron generation time. The delayed neutron fraction refers to neutrons which are produced by fission products called precursors. The average energy of delayed neutrons is lower than prompt neutrons and they have important role on controlling fission chain reaction (Van Dam et al., 2005). The larger effective delayed neutron fraction leads to slower reactor response. In order to calculate effective delayed neutron fraction, a prompt method (Farkas et al., 2008) is utilized in MCNPX2.6 code. In this method, the effective delayed neutron fraction is calculated as below:

$$\beta_{\text{eff}} = 1 - \frac{k_p}{k_{\text{eff}}} \tag{1}$$

where k_{eff} is the effective multiplication factor which is calculated by total number of neutrons in fission process including prompt and delayed neutrons. Also, k_p represents the effective multiplication factor considering prompt neutrons. In calculation of k_p, the effect of delayed neutrons is ignored. The prompt neutron generation time as another important kinetic parameter indicates the time for reactor to produce new generation of neutrons. The prompt neutron generation time is calculated using Eq. (2):

$$\Lambda = \frac{l_p}{k_{\text{eff}}} \tag{2}$$

where l_p is the prompt removal lifetime reported by MCNPX2.6 code.

Reactor core behavior dependency on the neutronic safety parameters is evaluated in the second step. For this purpose, RIA is selected as a transient case. The six-group point kinetic equations are applied to model the dynamic response of reactor core. In this approach, temperature reactivity coefficients are considered based on average temperature of fuel, clad and coolant in the core using lumped model. The lump model assumes a uniform temperature distribution for each component in the reactor core and subsequently simplifies calculation of the average temperatures for all the components. The following set of Eqs. (3) to (9) are used to model the reactor behavior:

$$\frac{\mathrm{d}n_r(t)}{\mathrm{d}t} = \frac{\rho(t) - \beta_{\text{eff}}}{\Lambda} n_r(t) + \sum_{i=1}^{6} \lambda_i C_i(t) \tag{3}$$

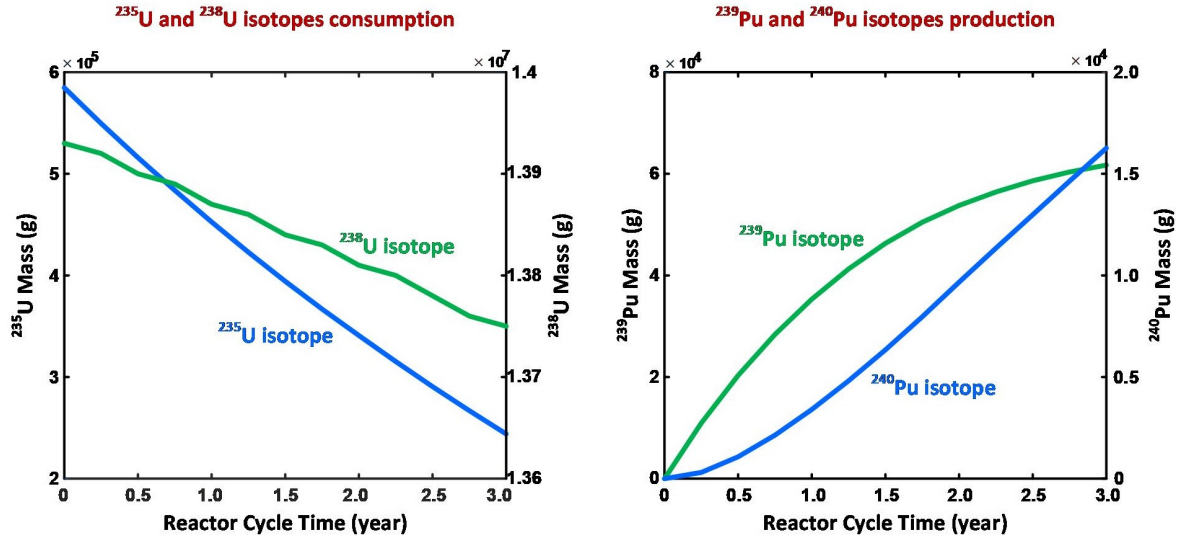

Figure 2: Fuel isotopic composition versus reactor cycle time.

$$\frac{\mathrm{d}C_i(t)}{\mathrm{d}t} = \frac{\beta_{\mathrm{eff},i}}{\Lambda} n_r(t) - \lambda_i C_i(t) \tag{4}$$

The time dependent reactivity is defined as:

$$\rho(t) = \rho_{\mathrm{inserted}}(t) + \rho_{\mathrm{feedback}}(t)(T_{\mathrm{fuel}}, T_{\mathrm{mod}}) \tag{5}$$

The RIA is evaluated at beginning and end of cycle for both HFP and HZP operational states. To provide an equal condition for comparison of neutronic safety parameters, the same time dependent reactivity insertion is assumed for all states as below:

$$\rho_{\mathrm{inserted}}(t) = \begin{cases} 400t\,(\mathrm{pcm}) & t \le 0.5\,\mathrm{s} \\ 200\,(\mathrm{pcm}) & t > 0.5\,\mathrm{s} \end{cases} \tag{6}$$

Total feedback reactivity is derived using following equation:

$$\begin{aligned} \rho_{\mathrm{feedback}}(T_{\mathrm{fave}}, T_{\mathrm{Cool}}) =& \alpha_{\mathrm{Cool}}(T_{\mathrm{Cool}})\Big[T_{\mathrm{Cool}} - T_{\mathrm{Cool}\,0}\Big] \\ &+ \alpha_f(T_{\mathrm{fave}})\Big[T_{\mathrm{fave}} - T_{\mathrm{fave}\,0}\Big] \end{aligned} \tag{7}$$

The fuel, clad and coolant (moderator) average temperatures in the core are calculated using energy conservation law as follows:

$$\frac{\mathrm{d}T_{\mathrm{fave}}}{\mathrm{d}t} = \frac{1}{M_f C_f}\Big(S_f P_0 n_r(t) - h_g A_g\big[T_f(R_f) - T_{\mathrm{Clad}}\big]\Big) \tag{8}$$

$$\begin{aligned} \frac{\mathrm{d}T_{\mathrm{Clad}}}{\mathrm{d}t} =& \frac{1}{M_{\mathrm{Clad}} C_{\mathrm{Clad}}}\Big(h_g A_g\big[T_f(R_f) - T_{\mathrm{Clad}}\big] \\ &- h_{\mathrm{Cool}} A_{\mathrm{Cool}}\big[T_{\mathrm{Clad}} - T_{\mathrm{Cool}}\big]\Big) \end{aligned} \tag{9}$$

$$\begin{aligned} \frac{\mathrm{d}T_{\mathrm{Cool}}}{\mathrm{d}t} =& \frac{1}{M_{\mathrm{Cool}} C_{\mathrm{Cool}}}\Big([1 - S_f] P_0 n_r(t) \\ &+ h_{\mathrm{Cool}} A_{\mathrm{Cool}}\big[T_{\mathrm{Clad}} - T_{\mathrm{Cool}}\big] \\ &- M^0_{\mathrm{Cool}} C_{\mathrm{Cool}}\big[T_{\mathrm{out}} - T_{\mathrm{in}}\big]\Big) \end{aligned} \tag{10}$$

The equations are solved using MATLAB software. More explanations about the mentioned method are described by Kamalpour et al. (Kamalpour et al., 2018).

The main reactor thermal-hydraulic parameters in HFP and HZP operational states are listed in Table 3.

Table 3: Reactor thermal-hydraulic parameters in HFP and HZP states in normal operational condition.

Parameter	HFP	HZP
Power ($\mathrm{MW_{th}}$)	330	1×10^{-3}
$\mathrm{T_{fcenter}}(K)$	964.7	
$\mathrm{T_{fave}}(K)$	854.4	568.8
$\mathrm{T_{Clad}}(K)$	601.9	
$\mathrm{T_{Cool}}(K)$	581.9	

4 Results and discussion

4.1 Fuel composition change during reactor cycle

SMART reactor utilizes ceramic UO_2 fuel with enrichment lower than 5 w/o. Figure 2 shows the variation of main isotopic compositions of fuel during reactor cycle. The U-235 isotope in fuel composition undergoes fission reaction with thermal neutrons and decreases continuously to sustain fission chain reaction. The other isotope, U-238, can either have fission with (high energy) fast neutrons or capture a slow neutron to produce Pu-239. Several fissile and fertile isotopes such as Pu-239, Pu-240, etc. are generated according to transmutation process (Shusterman, 2021). These isotopes contribute to fraction of thermal or fast fissions, particularly at EOC. Consumption of U-235 and U-238 along with production of actinides change the fuel isotopic composition which in turn affect nuclear safety parameters.

4.2 Reactivity temperature coefficients during reactor cycle

Variation of FTC and MTC versus reactor cycle time are shown in Fig. 3. The FTC is the consequence of Doppler

broadening effect in U-238 and Pu-240 isotopes. The production of Pu-240 isotope (refer to Fig. 2) leads to increase of FTC absolute value during fuel consumption over reactor cycle time.

The absolute amount of MTC also increases during reactor cycle. This is the result of decrease in required soluble boron for achieving the critical state during reactor operation time.

It should be noted that both FTC and MTC are negative during reactor operation time which demonstrate reactor inherent safety. However, variation of these coefficients during reactor cycle have significant influence on reactor behavior under RIA which is described in following sections. The FTC and MTC also depends on temperature change intervals. The FTC values in consecutive temperature intervals are gathered in Table 3 for range of 293 K to 1773 K. The results show that reactivity variation per fuel temperature change is larger in lower fuel temperatures. Table 4 represents the MTC values versus temperature intervals in the range of 293 K to 615 K. Change of moderator temperature leads to larger reactivity variation in higher moderator temperatures.

4.3 Kinetic parameters during reactor cycle

The influence of fuel burnup on effective delayed neutron fraction and neutron generation time is shown in Fig. 4. In general, the delayed neutron fraction produced by Pu-239 is smaller than U-235 (Akbari et al., 2018). This figure shows that effective delayed neutron fraction decreases with U-235 consumption and increase of Pu-239 role in fission reactions during reactor operation time.

Neutron absorption probability in BOC is larger than EOC according to higher fissile inventory in the core. This fact leads to smaller neutron lifetime and consequently smaller neutron generation time in BOC compared to EOC. Results show that neutron generation time increases from 16.4 μs in BOC to 25.8 μs in EOC.

4.4 Reactor dynamic response under RIA

In this section, reactor behavior is evaluated at BOC and EOC for both HFP and HZP operational states under reactivity insertion accident. It is considered that reactor is operating at steady state condition before accident initiation. A ramp reactivity insertion is modelled according to Eq. (6). Reactor scram is not actuated to demonstrate the effect of neutronic safety parameters on reactor behavior during RIA. Figure 5 illustrates the feedback effect at BOC and EOC for both HFP and HZP states upon reactivity insertion accident. As expected, fuel feedback reactivity response to input reactivity is faster than coolant feedback reactivity. This is the result of instantaneous increase in fuel temperature as power increases. The fuel center, clad and coolant average temperatures in the core versus time during RIA are plotted in Fig. 6.

Table 4: MTC values in different temperature intervals.

Temperature intervals		MTC (pcm.K^{-1})	
T1 (K)	T2 (K)	BOC	EOC
293	323	-0.10	-0.66
323	373	-1.04	-1.86
373	423	-1.60	-3.82
423	473	-2.58	-5.15
473	523	-4.11	-12.18
523	573	-8.41	-23.04
573	615	-19.67	-39.72
Average (293 K-615 K)		-5.88	-13.67

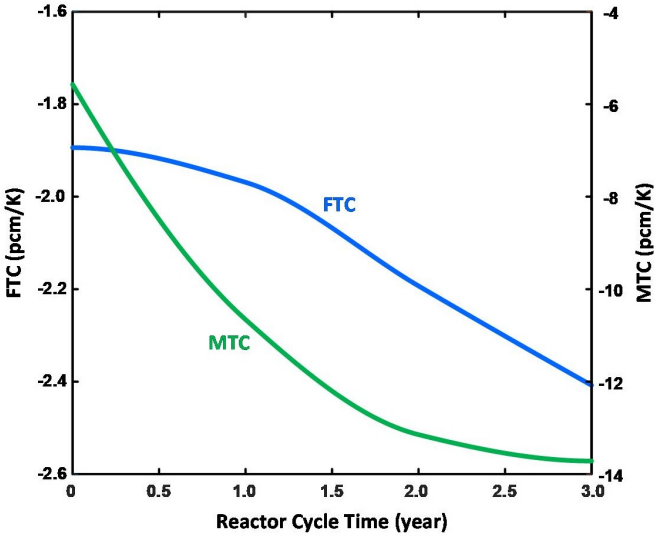

Figure 3: Reactivity temperature coefficients versus reactor cycle time.

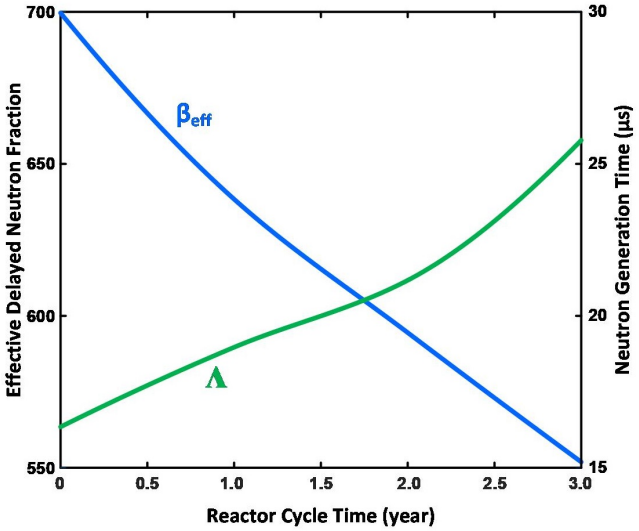

Figure 4: Reactor kinetic parameters change versus reactor cycle time.

The increase rates of fuel and coolant temperatures at HZP state are significantly smaller (refer to Fig. 6 and Table 5) than HFP state under RIA. Therefore, it takes longer time for arising feedbacks effect as a result of reactivity insertion in reactor at HZP state compared to reactor at HFP state.

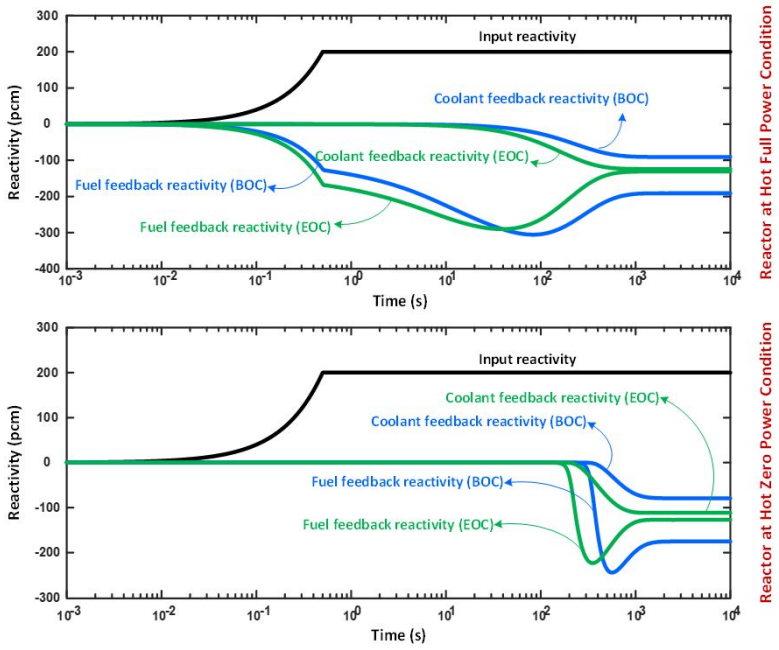

Figure 5: Feedbacks reactivity effect during RIA.

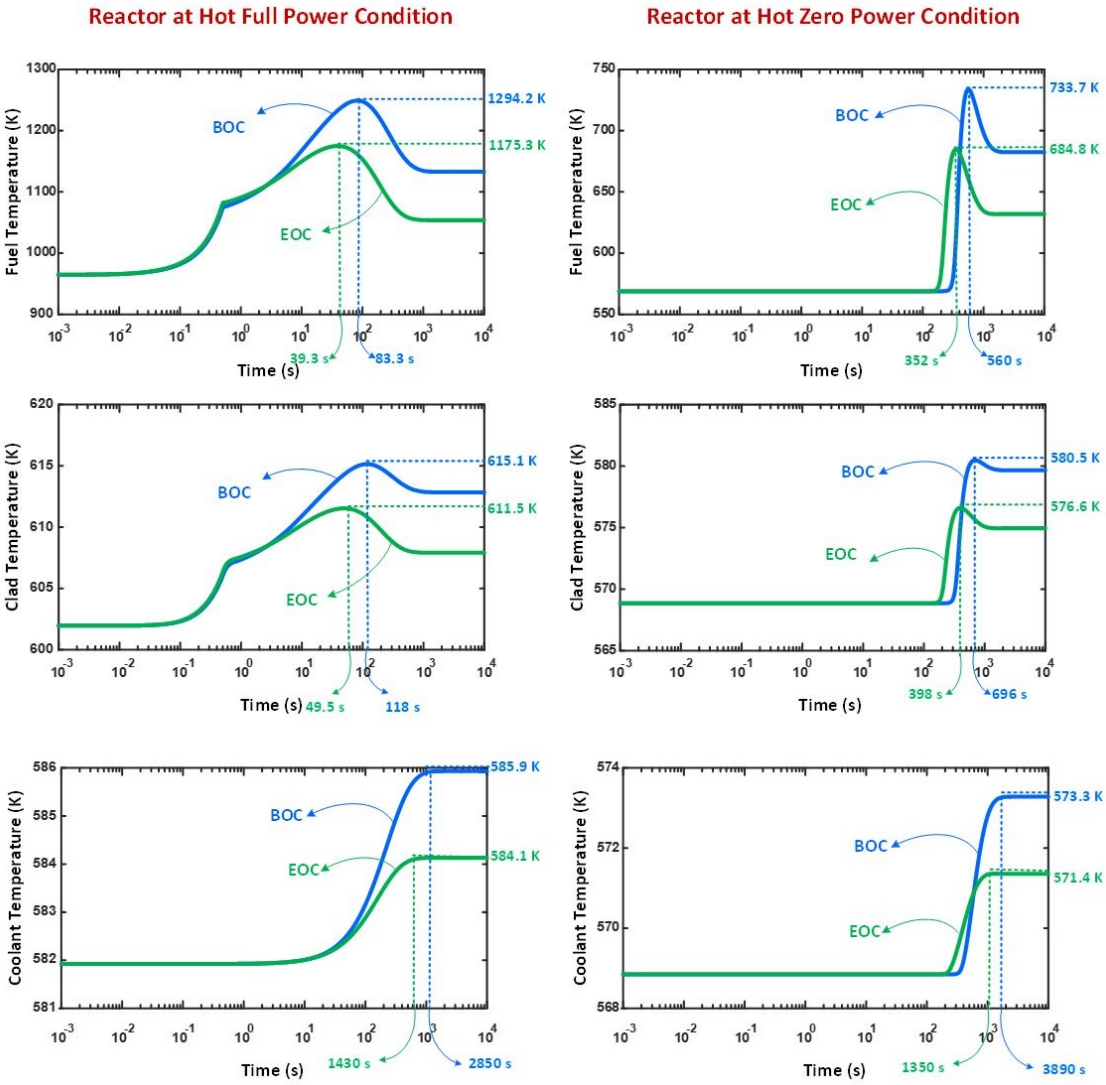

Figure 6: Average temperature of fuel, clad and coolant during RIA.

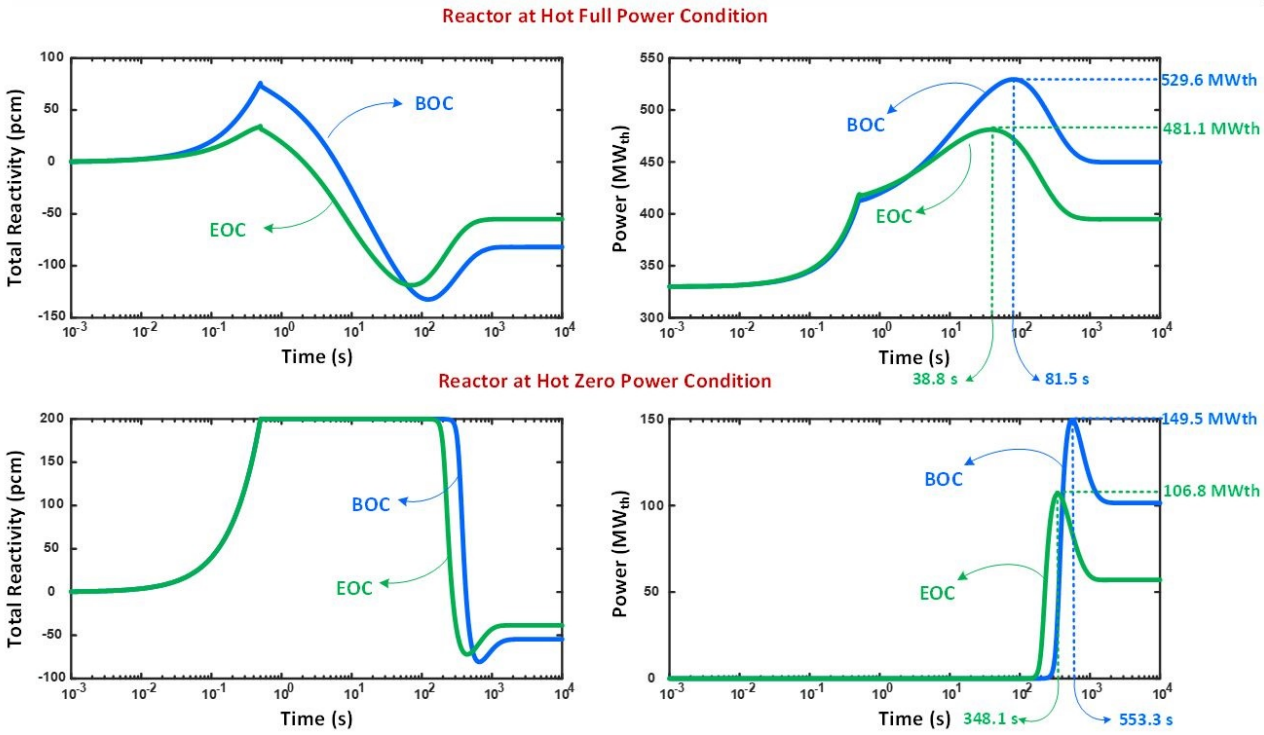

Figure 7: Power and total reactivity transients during RIA.

Table 5: The maximum reactor thermal-hydraulic parameters during RIA.

Reactor operational state		Max. power (time*) (MW_{th} (s))	Max. $T_{fcenter}$ (time) (K (s))	Max. T_{Clad} (time) (K (s))	Max. T_{Cool} (time) (K (s))
HZP	BOC	149.5 (553.3)	733.7 (560.0)	580.5 (696.0)	573.3 (3890.0)
	EOC	106.8 (348.1)	684.8 (352.0)	576.6 (398.0)	571.4 (1350.0)
HFP	BOC	529.6 (81.5)	1294.2 (83.3)	615.1 (118.0)	585.9 (2850.0)
	EOC	481.1(38.8)	1175.3 (39.3)	611.5 (49.5)	584.1 (1430.0)

*The time at which the parameter achieves its maximum value.

Reactor dynamic response corresponds to both feedbacks effect and kinetic parameters. As demonstrated in Fig. 3, FTC and MTC become stronger over reactor cycle time. It means that the absolute value of both FTC and MTC are larger at EOC than BOC. Therefore, it is expected that larger negative feedback reactivity at EOC leads to lower power increase compared to BOC.

The effective delayed neutron fraction decreases over reactor cycle time (refer to Fig. 4). In other words, larger fraction of fission neutrons are prompt neutrons at EOC in comparison with BOC. Therefore, reactivity insertion causes faster reactor response at EOC compared to BOC. On the other hand, neutron generation time becomes larger over reactor cycle time (refer to Fig. 4). This leads to lower power rate increase at EOC compared to BOC.

Figure 7 illustrates the total reactivity and reactor power during 1×10^4 seconds after accident initiation. The reactor power increases with reactivity insertion. Feedbacks arises to damp the positive reactivity effect and reactor reaches stability at new power level. The total reactivity plotted in Fig. 7 is obtained from Eq. (7). The amount of total core reactivity is zero during reactor normal operation. After reactivity insertion, the amount of total reactivity changes and finally reaches to a new constant reactivity. This reactivity which has a negative value indicates the reactivity loss in reactor system compared to initial state. This loss of reactivity is due to achievement of a higher stable level of power after reactivity insertion. Note that core reactivity is zero in the new power level. The maximum and stable thermal-hydraulic parameters of reactor during RIA are gathered in Tables 5 and 6, respectively. Following, the effect of feedbacks and kinetic parameters at BOC and EOC on SMART reactor behavior are described.

The reactivity insertion causes higher power peak at BOC compared to EOC for both HZP and HFP operational states. This is the result of stronger negative feedback reactivity and larger neutron generation time at EOC. In the HFP state, reactor reaches the maximum transient power of 529.6 MW_{th} at BOC and 481.1 MW_{th} at EOC. The transient peak of power at HZP state is smaller than HFP sate. The maximum transient power of reactor in HZP state at BOC and EOC are 149.5 MW_{th} and 106.8 MW_{th}, respectively.

The power peak occurs at shorter time after accident

Table 6: The reactor thermal-hydraulic parameters at 1×10^4 s after accident initiation.

Reactor operational state		Power (MW_{th} (s))	$T_{fcenter}$ (K)	T_{Clad} (K)	T_{Cool} (K)
HZP	BOC	101.4	682.4	579.6	573.2
	EOC	57.0	631.9	574.9	571.3
HFP	BOC	449.7	1132.9	612.8	585.9
	EOC	394.8	1053.7	607.9	584.1

initiation at EOC compared to BOC, according to smaller effective delayed neutron fraction. The time difference between BOC and EOC transient power peaks are around 43 s and 205 s for HFP and HZP operational states, respectively.

5 Conclusion

The reactor dynamic response dependency on neutronic safety parameters is an important issue for reactor reliable operation. Among neutronic parameters, MTC and FTC have the major effect on maintaining reactor stability during RIA. The negative feedbacks prevent excessive increase of power due to reactivity insertion. On the other hand, kinetic parameters specify the time scale of reactor response and reactor power change rate. The main purpose of the present study is to investigate SMART reactor behavior based on different set of neutronic parameters in BOC and EOC at both HFP and HZP reactor operational states. For this purpose, neutronic safety parameters of SMART are calculated during reactor cycle using MCNPX2.6 nuclear code. These parameters are employed in reactor dynamic model to predict reactor behavior during RIA. The reactor dynamic model is developed based on point kinetic equations and lumped temperature model using MATLAB software.

A comparative study of RIA in different reactor cases shows that negative feedbacks maintain reactor safe condition at all states. However, the feedbacks worth along with kinetic parameters value have significant influence on reactor behavior during reactor cycle. The following points are obtained from the results:

- The feedbacks effect becomes stronger over reactor cycle time which leads to smaller transient power peak at EOC compared to BOC in both HFP and HZP states. The reactor at EOC also stabilizes to a lower power level than BOC after accident initiation.
- The comparison of reactor response at different states shows that reactor in EOC at HFP operational state has the faster response to RIA among other examined states. The transient power peak of 481.1 MW_{th} take place in 38.8 s after accident initiation.
- The comparative study of same reactivity insertion (200 pcm/0.5 s) indicates that reactor experiences higher power and temperature transients at HFP rather than HZP. Note that the possibility of accident with higher reactivity insertion at HZP is greater than HFP, since higher number of control rod banks presents in the core at HZP state.

References

Akbari, M., Rezaei, S., and Khoshahval, F. (2018). Kinetic parameters calculation during first cycle of the WWER-1000 reactor core. *CNL Nuclear Review*, 8(1):63–70.

CNSC (2003). *Science and Reactor Fundamentals - Reactor Physics*. Canadian Nuclear Safety Commission. https://canteach.candu.org/content%20library/20030101.pdf.

Farkas, G., Michálek, S., and Haščık, J. (2008). MCNP5 delayed neutron fraction (β_{eff}) calculation in training reactor VR–1. *Journal of Electrical Engineering*, 59(4):221–224.

Hunt, B. R., Lipsman, R. L., and Rosenberg, J. M. (2014). *A guide to MATLAB: for beginners and experienced users*. Cambridge university press.

Ingersoll, D. T. and Carelli, M. D. (2015). *Handbook of small modular nuclear reactors*. Woodhead Publishing.

Kamalpour, S., Salehi, A. A., Khalafi, H., et al. (2018). The potential impact of Fully Ceramic Microencapsulated (FCM) fuel on thermal hydraulic performance of SMART reactor. *Nuclear Engineering and Design*, 339:39–52.

Kamalpour, S., Salehi, A. A., Khalafi, H., et al. (2019). Impact of integral burnable absorbers on SMART reactor behaviour under normal and anomalous operational conditions. *Progress in Nuclear Energy*, 110:51–63.

Lee, W. (2010). *The SMART reactor*. 4^{th} Annual Asian-Pacific Nuclear Energy Forum.

Louis, H. K. (2021a). Assessment of neutronic safety parameters of VVER-1000 core under accident conditions. *Progress in Nuclear Energy*, 132:103609.

Louis, H. K. (2021b). Sensitivity analysis of the kinetic parameters to physical parameters variation in VVER reactor. *Nuclear and Particle Physics*, 11:15–26.

MacFarlane, R. and Muir, D. (1994). *The NJOY Nuclear Data Processing System*. Los Alamos National Laboratory LA-12740-M.

Pelowitz, D. (2008). MCNPX User's Manual. Technical report, LA-CP-07-1473 Version 2.6. 0. Los Alamos, NM: US Department of Energy.

Pinem, S., Sembiring, T. M., Sunaryo, G. R., et al. (2018). Reactivity coefficient calculation for AP1000 reactor using the NODAL3 code. In *Journal of Physics: Conference Series*, volume 962, page 012057. IOP Publishing.

Reda, S. M., Gomaa, I. M., Bashter, I. I., et al. (2021). Neutronic performance of the VVER-1000 Reactor Using Thorium Fuel with ENDF Library. *Science and Technology of Nuclear Installations*, 2021.

Shusterman, J. (2021). *Fissile and fertile fuels, Volume 1*. Encyclopedia of Nuclear Energy.

Stankovskiy, A. and Van den Eynde, G. (2012). Advanced method for calculations of core burn-up, activation of structural materials, and spallation products accumulation in accelerator-driven systems. *Science and Technology of Nuclear Installations*, 2012.

Torabi, M., Lashkari, A., Masoudi, S. F., et al. (2018). Neutronic analysis of control rod effect on safety parameters in Tehran Research Reactor. *Nuclear Engineering and Technology*, 50(7):1017–1023.

Van Dam, H., Van der Hagen, T., and Hoogenboom, J. (2005). Nuclear reactor physics. *Delft University of Technology, Department of Nuclear Engineering*.